



RESEARCH LETTER

10.1002/2017GL076587

Key Points:

- An anomalously thick and persistent ice pack along the east coast of Canada in spring 2017 created hazardous maritime conditions
- Within one sea ice season multiyear sea ice from the Lincoln Sea and Canadian Arctic was advected southward to the coast of Newfoundland
- An increasingly mobile Arctic ice pack is increasing ice flux through Nares Strait and releasing more ice hazards toward southern locations

Supporting Information:

- Data Set S1
- Data Set S2
- Supporting Information S1

Correspondence to:

D. G. Babb,
david.babb@umanitoba.ca

Citation:

Barber, D. G., Babb, D. G., Ehn, J. K., Chan, W., Matthes, L., Dalman, L. A., et al. (2018). Increasing mobility of high Arctic Sea ice increases marine hazards off the east coast of Newfoundland. *Geophysical Research Letters*, 45, 2370–2379. <https://doi.org/10.1002/2017GL076587>







Received 28 NOV 2017

Accepted 22 FEB 2018

Accepted article online 28 FEB 2018

Published online 15 MAR 2018

Increasing Mobility of High Arctic Sea Ice Increases Marine Hazards Off the East Coast of Newfoundland

D. G. Barber¹, D. G. Babb¹ , J. K. Ehn¹, W. Chan¹, L. Matthes¹ , L. A. Dalman¹ , Y. Campbell¹, M. L. Harasyn¹ , N. Firoozy¹ , N. Theriault¹, J. V. Lukovich¹ , T. Zagon², T. Papakyriakou¹, D. W. Capelle¹, A. Forest³, and A. Gariepy⁴

¹Centre for Earth Observation Science, University of Manitoba, Winnipeg, Manitoba, Canada, ²Canadian Ice Service, Ottawa, Ontario, Canada, ³Amundsen Science, Laval University, Quebec, Quebec, Canada, ⁴Canadian Coast Guard, Quebec, Quebec, Canada

Abstract Heavy ice conditions along Canada's east coast during spring 2017 presented hazardous conditions for the maritime industry and required the Canadian Coast Guard to pull its research icebreaker, CCGS *Amundsen*, off its scientific cruise to provide ice escort services and conduct search and rescue operations along Newfoundland's northeast coast. Greater ice concentrations and a thicker ice pack than are typical of this area created the anomalous ice cover. Within this paper we present in situ observations of the ice cover, confirming that pieces of multiyear sea ice from the high Arctic were present within the ice cover, and subsequently examine the transport pathway that connects the export of thick multiyear sea ice from the Lincoln Sea and Canadian Arctic Archipelago to coastal communities in Newfoundland. We conclude with a discussion on how an increasingly mobile Arctic sea ice cover may increase these ice hazards in the south.

Plain Language Summary Heavy ice conditions along Canada's east coast during spring 2017 presented hazardous conditions for the maritime industry at a time of year when vessels typically do not need to contend with sea ice. Greater ice concentrations and a thicker ice pack than are typical of this area created the anomalous ice cover. Our in situ observations from aboard the Canadian ice breaker *Amundsen* confirm that multiyear sea ice from the High Arctic was present and that two storms in late March compressed this thick ice cover onshore, where it persisted into late July. Within this work we connect the export of thick multiyear sea ice from the High Arctic and Canadian Arctic Archipelago to downstream areas where this thick multiyear ice cover is advected during winter. As the Arctic ice pack has declined in aerial extent and thickness, it has become increasingly mobile. This has contributed to increased ice transport through narrow channels along the periphery of the Arctic Ocean (i.e., Bering Strait, Nares Strait, and interisland straits of the Canadian Arctic Archipelago) and increased the presence of thick multiyear sea ice from the High Arctic at more southern locations that have typically not contended with such sea ice.

1. Introduction

Sea ice is typically present along the northeast coast of Newfoundland from mid-January to early May with an ice cover that is predominantly composed of first-year ice (FYI) types, while a small portion of multiyear ice (MYI) that has been advected southward from Baffin Bay is also typically present (Canadian Ice Service, 2011; hereafter CIS, 2011). However, an anomalously thick ice cover remained present around Newfoundland during May and June 2017, a time of year when marine vessels normally operate unimpeded by sea ice. The sea ice presented a risk for maritime operations in the area and even sank two fishing vessels beset within the ice cover. As a result, the Canadian Research icebreaker CCGS *Amundsen* was diverted from its scientific mission in Hudson Bay to the east coast of Newfoundland, where it escorted ferries, resupplied vessels and tankers through the ice cover, conducted search and rescue operations for fishing vessels beset in the ice, and provided aerial reconnaissance with its helicopter. In between Coast Guard operations, the science crew aboard took advantage of the situation and collected in situ observations of the physical and electromagnetic properties of the unusually thick sea ice. Within this paper, we present in situ observations of the geophysical properties of the anomalous ice cover, provide historical context of sea ice within the study area, and focus on how this unusual ice cover came to be present around Newfoundland.

The cold temperate climate around Newfoundland limits local ice growth to new and gray ice types during winter. However, northwesterly winds coupled with the southeastward flowing Labrador Current advect

thicker sea ice from Baffin Bay through the Labrador Sea toward Newfoundland throughout winter (Fissel & Tang, 1991; Symonds, 1986). Along the Labrador coast the ice cover is aligned in parallel bands, with thinner, locally formed ice types closer to shore and thicker pack ice from Baffin Bay drifting in an outer band open to the ice edge (Prinsenber & Peterson, 1992). Around Newfoundland, the thinner coastal ice ranges in thickness from 0.1 to 0.5 m, while the thicker outer band ranges in thickness from 1.0 to 4.0 m (Fissel & Tang, 1991; Prinsenber et al., 1996). The ice cover has a maximum southern limit of 47°N (Fissel & Tang, 1991; Tang, 1991), while the eastern extent of the ice cover is highly dependent on surface winds. The typical westerly wind direction disperses the ice cover into the offshore area, while cyclones passing Newfoundland drive easterly winds that compress the ice cover into coastal regions (Han et al., 2015). The influence of these storm events is compounded by a low internal ice stress field that makes the ice cover more responsive to winds (Fissel & Tang, 1991) and fosters peak ice drift speeds of up to 75 km d⁻¹ during storms (Prinsenber & Peterson, 1992).

The thicker pack ice present in the outer band of the ice cover offshore of Newfoundland comes from the upstream area of Baffin Bay. Baffin Bay is typically ice covered from October to August with ice-free conditions present throughout most of the Bay during summer (CIS, 2011). Following the onset of sea ice formation in northern Baffin Bay during September and October, the ice cover advances southward due to both the formation of new ice, as well as the southward advection of the existing ice cover under southerly winds driven by a persistent atmospheric trough (CIS, 2011; Kwok, 2007). The ice cover in Baffin Bay is composed of a mix of FYI, which forms locally, and MYI that is advected into the Bay from either the Lincoln Sea via Nares Strait or from the Canadian Arctic Archipelago (CAA) through Jones or Lancaster Sound (locations labeled in Figure 3a). MYI is typically confined to western Baffin Bay, while FYI is present through eastern Baffin Bay, giving rise to the zonal difference in ice thickness within the Bay (Landy et al., 2017). Lancaster Sound exports an average of 68,000 km² yr⁻¹ into Baffin Bay, which is composed of a mix of FYI and MYI from within the CAA (Agnew et al., 2008). Meanwhile, the presence of ice arches in Nares Strait from January until June or July has historically limited ice export to 33,000 km² yr⁻¹ (Kwok, 2005), a majority of which is MYI (Kwok et al., 2010). However, due to declining sea ice concentration and thickness, the Arctic ice pack is becoming mechanically weaker, which has implications for ice arch formation. In 2007 an ice arch did not form across Nares Strait and as a result 87,000 km² of sea ice was exported (Kwok et al., 2010). The following year in 2008 the ice arch did not form until April and 77,000 km² of sea ice was advected through Nares Strait (Kwok et al., 2010). The lack of, and delayed formation of the ice arch during 2007 and 2008, respectively, was ascribed to the mechanical weakening of the Arctic ice pack as a result of declining sea ice extent, concentration, and thickness (Kwok et al., 2010). Similar observations have been made for the Bering Strait (Babb et al., 2013) and interisland straits of the CAA (Howell et al., 2013), while Rampal et al. (2009) and Spreen et al. (2011) also ascribed pan-Arctic increases in ice drift speeds to the mechanical weakening of the Arctic ice pack. In terms of Nares Strait, the increased ice flux is important because as a result of pan-Arctic patterns of ice drift, sea ice converges against the northern coast of Greenland and the CAA (Kwok, 2015), forming the thickest sea ice in the world (Bourke & Garrett, 1987). Within the Lincoln Sea, between 2004 and 2009, Haas et al. (2010) showed that the ice thickness distribution for all years was characterized by a long right tail, with an annual mean spring ice thickness of 4.37 to 5.78 m and an annual modal MYI ice thickness of 3.2 to 4.4 m. When the Nares Strait ice arch is not in place, it is this thick MYI that is flushed into Baffin Bay and advected downstream toward areas of maritime activity.

2. Methods

On 25 May 2017, the Canadian Research Icebreaker CCGS *Amundsen* left Quebec City bound for the first ever survey of Hudson Bay while the seasonal ice cover was still intact and freshwater runoff was at its annual peak as part of the Hudson Bay System Study (BaySys). In anticipation of sampling sea ice in Hudson Bay, the *Amundsen* was fully outfitted with instrumentation to sample the geophysical, thermodynamic, and electromagnetic properties of sea ice. Once the *Amundsen* was diverted to Newfoundland, in between Coast Guard operations, we were able to collect in situ geophysical and electromagnetic samples from three of the larger ice floes we encountered. The Kovacs Mark II ice coring system (9 cm diameter) was used to extract a partial core from Floes 1 (top 287 cm) and 2 (top 220 cm), while a full core was extracted from Floe 3 (439 cm). Temperature was measured immediately after the ice core was extracted with a digital thermometer and subsequently sectioned (10 cm intervals) and melted for conductivity measurements.

Electromagnetic properties of the three floes were measured with ship-mounted (i) infrared transducer (9–11 μm), (ii) passive microwave radiometers (19, 37, and 89 GHz), and (iii) polarimetric C-band scatterometer (5.5 GHz). The infrared transducer provided an estimate of the skin surface temperature; the passive radiometers and active scatterometer measure the dual-polarized brightness temperatures and the polarimetric normalized radar cross-section signatures respectively, at various incidence angles within a small footprint (1 to 2 m^2). Aerial surveys of two study sites were conducted with a DJI Phantom 4 drone. Images were geocorrected, and softcopy photogrammetry was used to create a mosaic over the study area, from which the floe size distribution was determined. The southward advection of MYI from the Lincoln Sea and CAA was tracked through weekly CIS ice charts (freely available online at <http://iceweb1.cis.ec.gc.ca/Archive/page1.xhtml?grp=Guest&lang=en>) that depict total and partial ice concentrations according to the World Meteorological Organization's egg code. We attempted to use remotely sensed fields of ice drift (OSI SAF global low-resolution ice drift product; Lavergne et al., 2010) to complement the advection of MYI; however, the ice drift speeds were considerably below speeds derived from the ice charts and provided very limited data south of Hudson Strait; as a result the data are only presented for context in Figure S1 in the supporting information. Daily fields of sea level pressure (SLP) and surface wind components were acquired from the National Centers for Environmental Prediction Reanalysis-2 product (Kalnay et al., 1996; Kanamitsu et al., 2002).

3. Results and Discussion

Sea ice was present within the study area from late November 2016 to mid-June 2017 (Figure 1). Icebergs and traces of new ice first entered the study area in late November when daily mean air temperatures fell below 0°C , although sea ice concentrations greater than trace amounts ($\geq 1/10$) were present only after early January (Figure 1b). The ice cover was predominantly composed of new ice during January, but concentrations of thin, medium, and eventually thick FYI increased throughout winter (Figure 1b). MYI was first advected into the study area on 27 February, roughly 4 weeks earlier than the 1997 to 2016 average date of March 24 (red line Figure 1c). The arrival of MYI in the study area is highly variable, ranging from 9 February 1998 to 9 May 2016 (Figure 1c), likely as a result of variable wind forcing and ice drift speeds in Baffin Bay and the Labrador Sea. The ice cover reached its maximum extent of 58,250 km^2 on 13 February when persistent cold temperatures drove the rapid areal expansion of new ice (Figure 1b). Daily mean air temperatures at St. Anthony, Newfoundland, remained below 0°C until late April, maintaining over 40,000 km^2 of sea ice throughout February, March, and April. In early May, the daily mean air temperature surpassed 0°C , indicating that sea ice melt had begun. In mid-May the sea ice area declined by 50% as thin and medium FYI types melted out first, while thick FYI and MYI persisted until the area became ice-free on 26 June. This is the latest that the study area had become ice-free in the last 21 years (1997–2017), during which the average date was 30 May (blue line Figure 1c) and is in part due to an anomalously high sea ice area during spring (Figure 1c). Furthermore, according to the CIS ice charts, the ice cover of early May was composed of more MYI than any other year, except for 2007; contained more thick FYI than any other year, except for 1997; and contained more medium FYI than any other year on record.

When the *Amundsen* entered the study area on 2 June, we encountered a compressed ice pack that was composed of slush ice, heavily broken small pieces of brash ice (< 5 m floe diameter), small floes (5–100 m floe diameter) of either dynamically deformed FYI or MYI, and intermittent icebergs (max height of approximately 15 m; Figure 2a). The ice cover displayed signs of advanced ice melt, such as melt holes and drained melt ponds, while also displaying a dynamic history with ridges and rafted pieces of ice. Aerial drone surveys reveal that ice floes greater than 1 m^2 covered 61% of the study area, while the remaining 29% was covered by heavily fractured floes less than 1 m^2 and slush ice (Figure 2b). Aerial surveys also provided evidence of much larger MYI floes that had broken into smaller floes (Figure 2a), likely as a result of swells propagating through the ice cover (i.e., Asplin et al., 2012). The three floes that we sampled were all less than 100 m along their longest axis and had point ice thicknesses of > 5 , 4.28, and 4.39 m, while an electromagnetic induction system provided bare ice thickness estimates over 6 m on each floe. Floe 1 had several interconnected melt ponds that were surrounded by bare ice (Figure 2d), while Floes 2 and 3 differed in their surface appearance with ridged and rafted pieces of ice as well as noninterconnected melt ponds (Figure 2c). Ice cores reveal that Floes 2 and 3 were isothermal at -0.2°C and completely fresh, save for a saline bottom 60 cm on Floe 3 (Figure 2e). Floe 1 was characterized by an inverted nonlinear temperature gradient, though the floe was

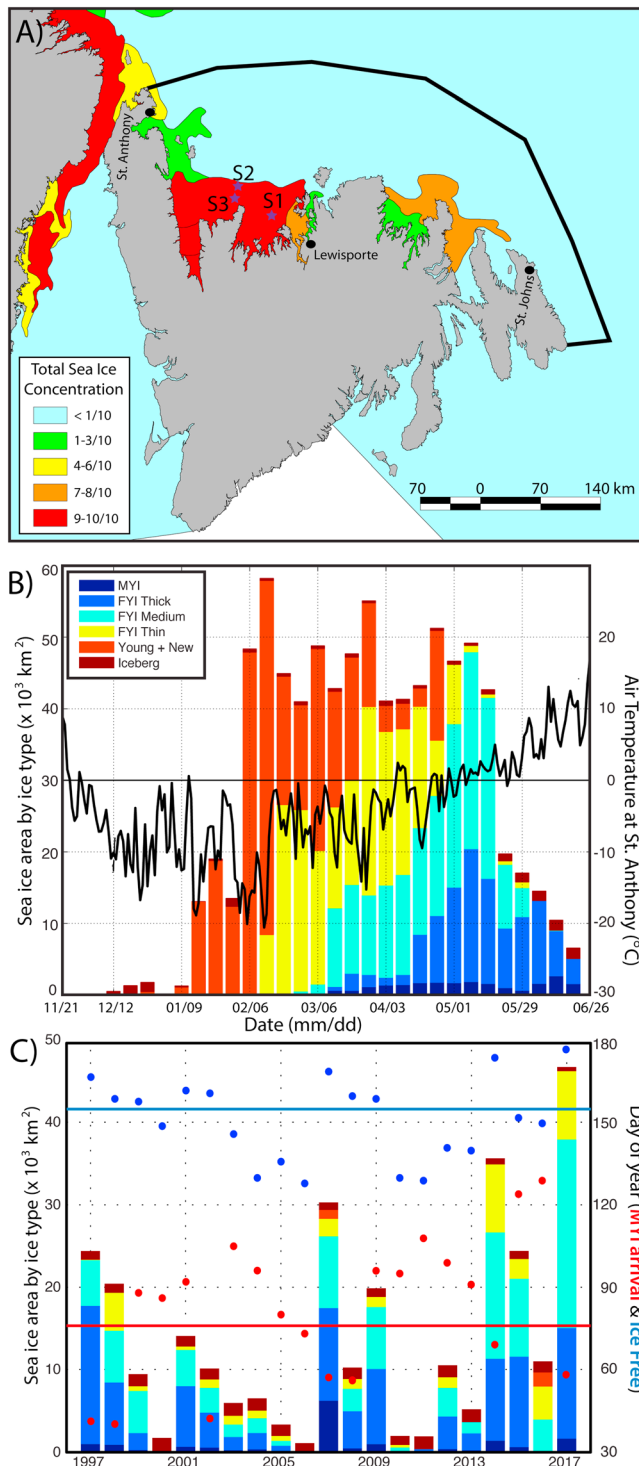


Figure 1. (a) Total sea ice concentration within the study area off the northeast coast of Newfoundland on 29 May 2017 with the three study sites marked. (b) Seasonal evolution of sea ice concentration, by ice type in the study area from weekly Canadian Ice Service ice charts between November 2016 and June 2017. The daily mean air temperature from the Environment Canada weather station at St. Anthony is overlaid. (c) Total ice concentration by ice type in the study area during the first week of May from 1997 to 2017. Overlaid by the day of year that multiyear ice entered the study area (red dots) and the day of year that the area became ice-free (blue dots), the mean for each is denoted by the horizontal line.

near the melting point. Beyond the visual and physical observations, the ship-based C-Band scatterometer measured cross-polarized ratios of -8.82 (HV/HH) and -8.09 dB (HV/VV), both of which correspond to MYI (Drinkwater et al., 1991; Kim et al., 2012). Ultimately, through a combination of visual, physical, and electromagnetic observations, we confirmed that thick MYI was present in the study area. Given that seasonal ice types are typical of the coastal study area, we next examine the source region of this MYI and the transport pathway that advected it toward the Newfoundland coast.

At the start of October 2016, Baffin Bay was almost completely ice-free (Figure 3), while MYI was present upstream in both Lancaster Sound and Nares Strait (Figure 3a). Beyond Nares Strait, MYI concentrations of nine tenths were present throughout the Lincoln Sea, and beyond Lancaster Sound, MYI was present within the CAA (Figure 3a). MYI was flushed through Nares Strait into Northern Baffin Bay during summer and fall 2016, until an ice arch formed across the mouth in January (European Space Agency, 2017; SF2 and SF3). During this time we speculate that reversals of the Beaufort Gyre to a cyclonic pattern (evident in SF2; purple shading SF4, after Lukovich & Barber, 2006) increased ice flux through Nares Strait by first diverging the Lincoln Sea ice cover northward and subsequently flushing MYI through the Strait when ice drift returned to the typical anticyclonic circulation (SF2 and SF4). According to the ice charts, MYI entering Baffin Bay through Nares Strait prior to the onset of freezeup in northern Baffin Bay during October would typically melt out, whereas MYI entering after freezeup had begun appears to persist within the ice pack. In terms of Lancaster Sound, FYI was the dominant ice type in the area throughout winter 2016–2017; however, MYI from upstream within the CAA was exported in concentrations from trace amounts to three tenths. The only exception to this occurred in early February when a large, MYI dominated (eight tenths) area of ice was exported through Lancaster Sound.

During October, freezeup began within northern Baffin Bay. FYI was the dominant ice type throughout the area, though MYI was present in concentrations of up to two tenths in western Baffin Bay (Figure 3b). By tracking the MYI that passed through Lancaster Sound during October within the ice charts we determined that the leading edge of MYI within Baffin Bay was composed of MYI from the CAA. However, once MYI from the Lincoln Sea reached the mouth of Lancaster Sound, it became impossible to distinguish MYI from the two regions. Therefore, in order to provide an approximate location of MYI from the Lincoln Sea, we manually tracked a MYI floe through 67 successive Sentinel images from 10 September 2016, when the floe was in the Lincoln Sea, to 10 March 2017 (yellow dots Figure 3), when the ice floe broke up at approximately 63°N , for a total drift of 2,581 km over the 150 day period.

Following the onset of freezeup during early October in northern Baffin Bay, the ice cover expanded southward quickly through winter. The leading ice edge had reached Hudson Strait by early December, while the MYI edge was just south of Davis Strait (Figure 3c). The ice edge expanded southward through December and January, with sea ice reaching Newfoundland by the end of February (Figures 1 and 3). South of Davis Strait, the MYI edge was stretched into an elongated tongue composed of trace amounts of MYI that had passed Hudson Strait in early January

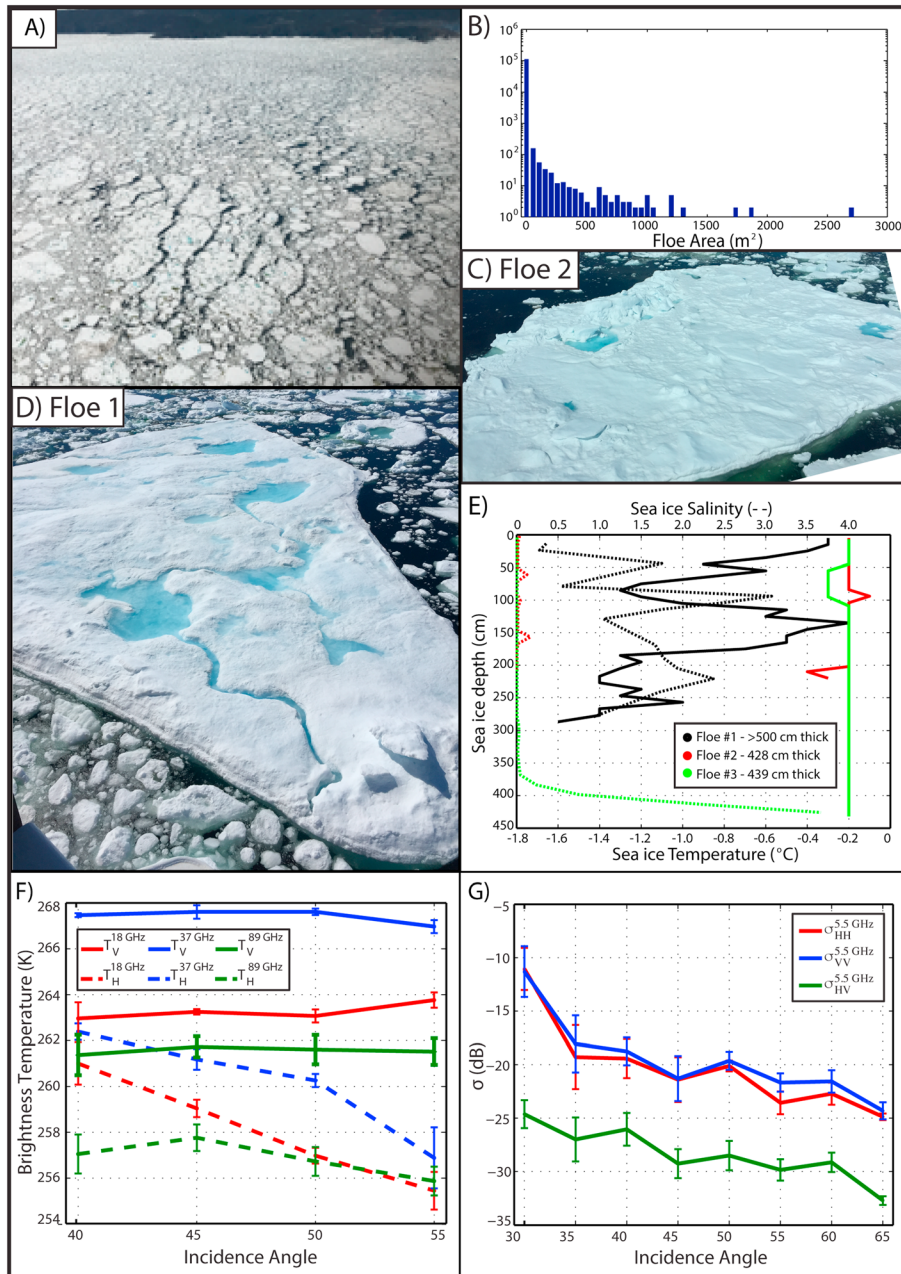


Figure 2. (a) Aerial shot of the ice pack within the study area. (b) Floe size distribution from a drone survey in the study area. (c) Floe 2. (d) Floe 1. (e) Temperature and salinity profiles of from the three ice floes sampled. (f) Passive and (g) Active microwave signatures from Floe 2.

and entered the study area at the end February (Figures 1 and 3). This is 4 weeks prior to the 1997–2016 average MYI arrival date of March 24 (Figure 1c), which is likely due to increased atmospheric forcing of ice drift through Baffin Bay and the Labrador Sea during late 2016 and early 2017.

Provided that MYI did not enter Baffin Bay until early October, we determine that it took 9 weeks for MYI from Lancaster Sound to reach Davis Strait and an additional 12 weeks to reach the study area around Newfoundland for a total travel time of 21 weeks. When MYI first entered the study area on 27 February, the MYI floe that we tracked from the Lincoln Sea was located just south of Davis Strait around 65°N. Assuming the floe drifted at speeds similar to the leading MYI edge, we speculate that the MYI floe from the Lincoln Sea would have arrived in the study area in mid-May. From this we determine that it takes

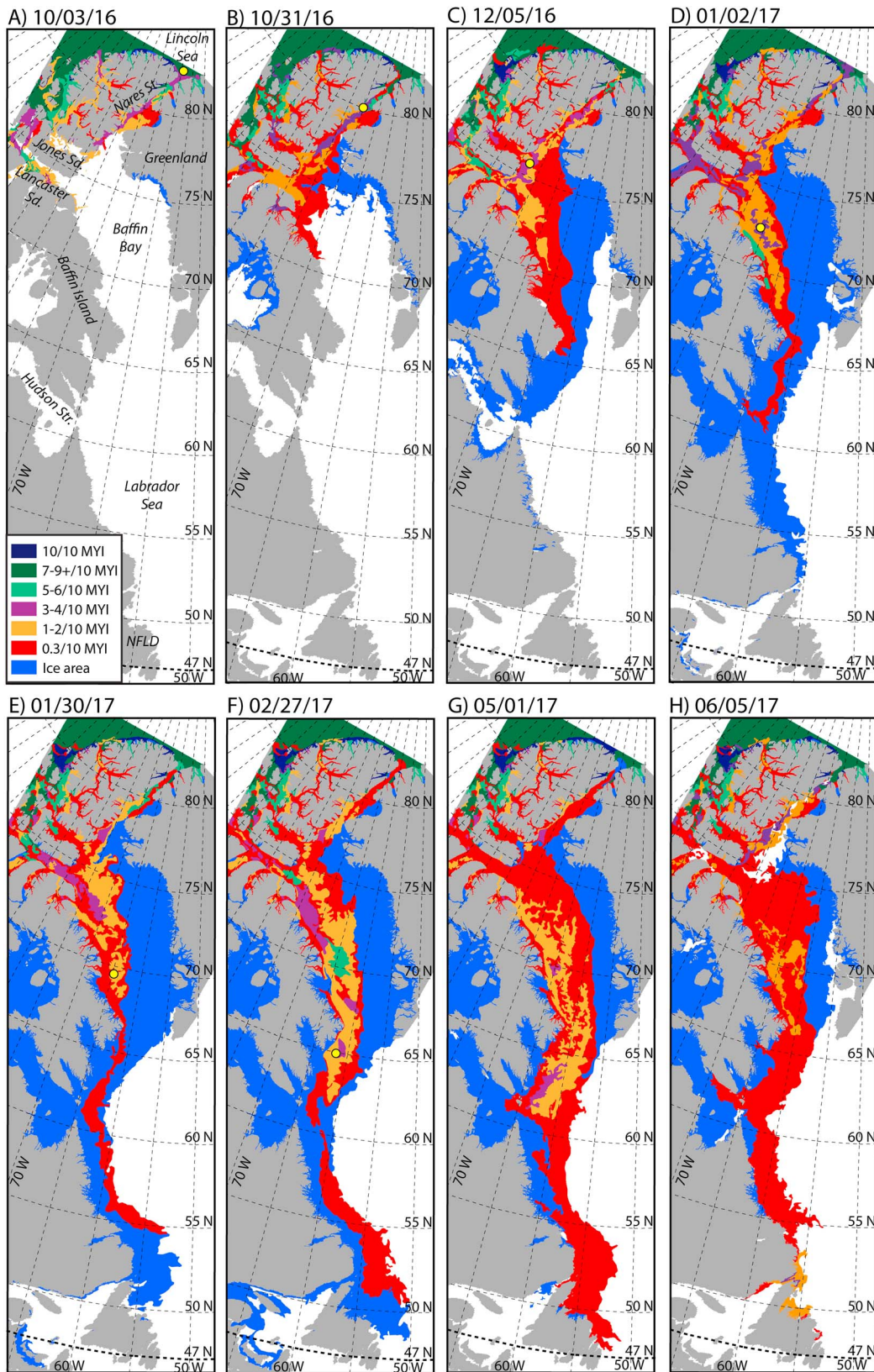


Figure 3. Monthly maps of sea ice extent and the partial concentration of multiyear ice (MYI) through the Eastern Canadian Arctic and east coast of Canada as presented within weekly ice charts from the Canadian Ice Service. The sea ice thermodynamic limit of 47°N is highlighted on each map. The yellow dots denote the position of a MYI floe that was manually tracked through successive Sentinel images from September 2016 to March 2017.

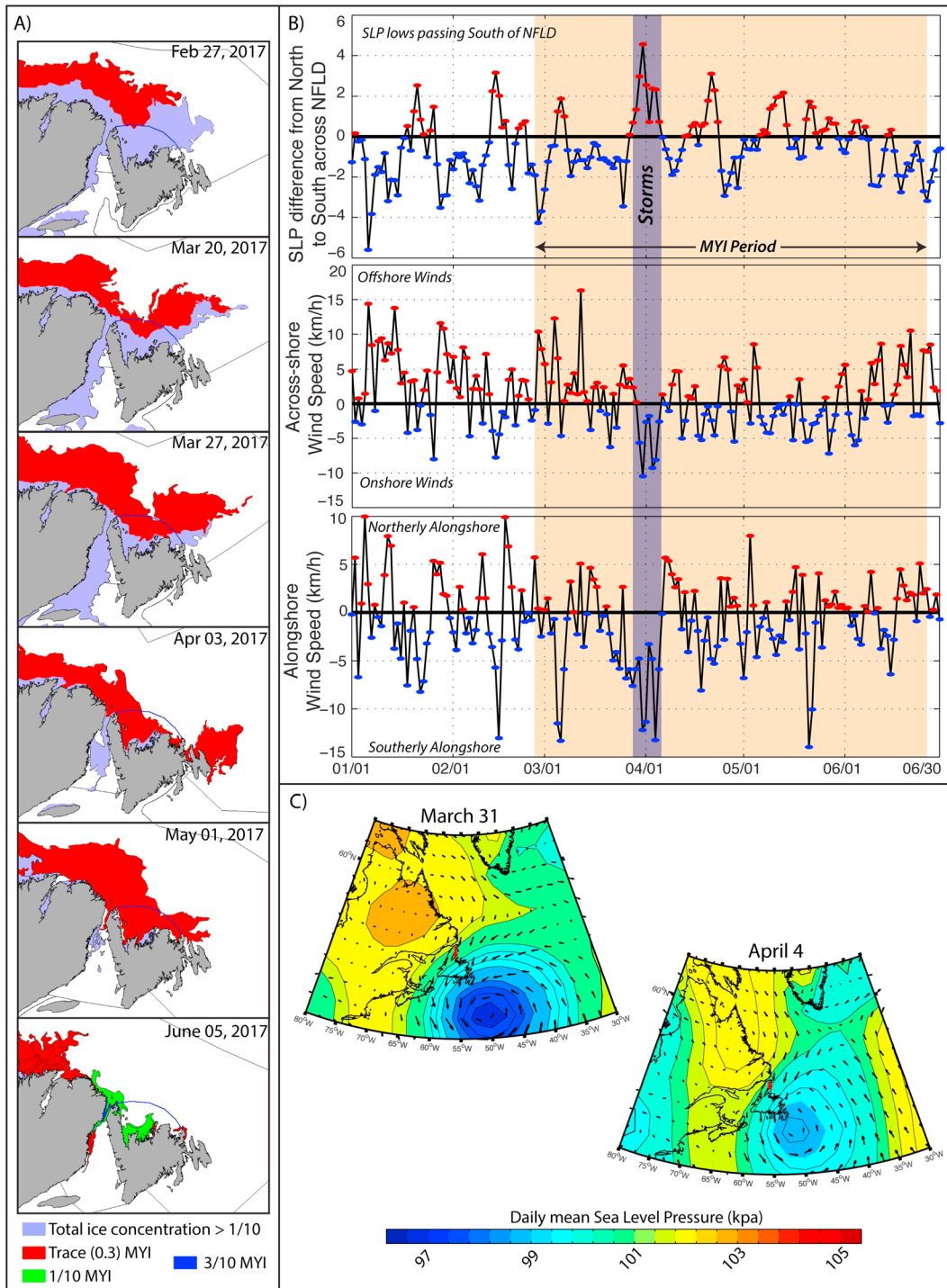


Figure 4. (a) Weekly multiyear ice (MYI) concentrations from Canadian Ice Service ice charts from 27 February, when MYI entered the study area (blue line), to 5 June when the *Amundsen* was operating in the area. Sea ice area presented in blue. (b) Time series of the sea level pressure (SLP) index rotated National Centers for Environmental Prediction (NCEP) wind components (on/offshore and north-northwest/south-southeast alongshore winds) from 1 January to 30 June. The MYI period is highlighted orange, and the period of MYI convergence on the coast is highlighted in purple. (c) Daily SLP and surface wind maps from NCEP reanalysis 2, with in situ winds from the Environment Canada station at St. Anthony, are also present in red. The maps highlight two storms that passed through the area in late March and early April 2017 and drove the MYI convergence.

32 weeks (~8 months) for MYI to travel the approximately 3,700 km (approximately 16.5 km d^{-1}) from the Lincoln Sea to the coastal waters around Newfoundland.

The timing of this departure is key because following the seasonal peak MYI extent in May (Figure 3g), the ice edge began to retreat, and by early June, the MYI tongue along the Labrador coast was no longer connected to the remnant MYI around Newfoundland (Figure 3h). Based on our observations we know that MYI was not present in Baffin Bay until the first week of October, and the transport path connecting the CAA and Lincoln Sea to Newfoundland was interrupted during early June. When combined with the observed transport time of 21 weeks, we determine that during the 2016–2017 sea ice season, MYI had to be advected through Lancaster Sound between early October and mid-January in order for it to represent a potential ice hazard around Newfoundland. In terms of MYI from the Lincoln Sea, we estimated a transport time of 32 weeks, 5 weeks of which are required for the floe to transit through Nares Strait (based on our manual tracking). Hence, MYI must enter Nares Strait between late August and late October in order for it to represent a potential ice hazard around Newfoundland. Ultimately, MYI entering Baffin Bay via Lancaster Sound prior to 1 October, or Nares Strait from the Lincoln Sea prior to late August, will melt out in Baffin Bay. Similarly, MYI entering Baffin Bay via Lancaster Sound after mid-January, or Nares Strait from the Lincoln Sea after late October, will not make it to Newfoundland before the MYI tongue is disrupted due to the onset of spring melt and the northward retreat of the ice edge.

Around the southerly latitudes of Newfoundland, MYI is usually offshore along the eastern periphery of the ice edge and drifts past Newfoundland toward the southern ice limit of 47°N (Fissel & Tang, 1991, Figure 3). Such was the case during February and March 2017 (Figure 4a), when MYI was only present in the eastern periphery of the ice cover. However, between 20 March and 3 April, trace amounts of MYI became present throughout the study area and subsequently persisted through spring, becoming more concentrated as the surrounding FYI melted out following the onset of melt in early May (Figures 1c and 4a). The convergence of MYI from the offshore area toward Newfoundland was driven by the passage of a large cyclone on 31 March (Figure 4c) that caused a seasonal peak in the northwest to southeast (NW-SE) SLP gradient across Newfoundland ($>4 \text{ kpa}$). A second cyclone passed the area on 4 April (Figure 4c) and maintained a positive NW-SE SLP gradient across Newfoundland (Figure 4b). Combined, the two storms drove persistent northeasterly winds over the study area between 28 March and 5 April (purple shading Figure 4b). This period was characterized by the seasonal peak in onshore wind speeds and strong alongshore winds that would have both converged the ice cover toward Newfoundland, while also drawing in more MYI from north of the study area. For context, between 1997 and 2016 during the MYI period (February to May from Figure 1c), the NW-SE SLP gradient across Newfoundland exceeded 4 kpa only 5 times, and all 5 times northeasterly winds compressed the ice cover against the northeast coast of Newfoundland. However, three of the storms (10 March 1999, 12 February 2010, and 2 March 2013) occurred prior to the MYI edge reaching the study area (Figure 1c); therefore, there was no MYI to advect shoreward with the onshore winds. Storms in March 1998 and 2006 forced MYI onshore though they had very different outcomes. The 1998 storm led to the fourth highest MYI area during early May, though sea ice melt proceeded rapidly and the area became ice-free around the average time (Figure 1c). Following the storm in March 2006 the MYI was compressed along the northern peninsula of Newfoundland, but the offshore ice cover was not replenished by the southward advection of sea ice from the Labrador Sea. This led to the lowest May ice area during the 21 year period and earliest onset of ice-free conditions (Figure 1c). Ultimately, the storms of 2017 occurred while MYI was in the offshore area and available to be advected onshore, but subsequently, the offshore ice cover was replenished by southward advection from the Labrador Sea, while regular onshore winds following the storm maintained the MYI cover within the study area (Figure 4b). Following melt onset in early May the seasonal ice cover preferentially melted out (Figure 1c) and thereby concentrated MYI (Figure 4a). Collectively, these factors fostered the compressed, wave-fractured MYI cover that persisted later into the season and presented hazardous conditions to maritime vessels during June and necessitated the use of the *Amundsen*.

4. Conclusions and Recommendations

During spring 2017 an anomalous ice cover composed of MYI from the High Arctic presented hazardous conditions off the northeast coast of Newfoundland. The ice cover was thicker than is typical of the area and as a result persisted into late June when the area is typically ice-free and maritime traffic can proceed

unimpeded by sea ice. In situ observations of the geophysical and electromagnetic properties of the ice cover confirmed that MYI was present within the ice cover, while complementary observations from ice charts and other spaceborne sensors reveal that these MYI floes were advected over 3,000 km from the Lincoln Sea and CAA to the coastal waters around Newfoundland within one ice season. Based on tracking the MYI edge, we determine that MYI must enter Baffin Bay through Lancaster Sound between early October and mid-January or enter Nares Strait from the Lincoln Sea between September and December in order to be transported to Newfoundland before the ice edge begins to retreat in early May. While it is typical for MYI to be advected southward through Baffin Bay and the Labrador Sea toward the southern ice edge, this ice is typically well offshore and melts out along the southern and eastern ice edges. However, in late March to early April 2017, two cyclones passed south of Newfoundland and drove the MYI floes into coastal areas where the ice cover remained present until it eventually melted out in late June. These storms created an unusually strong SLP gradient across Newfoundland and fostered strong onshore winds at a time of year when MYI was present in the offshore area.

Under a changing climate, the Arctic ice pack has become increasingly mobile, with increased ice drift speeds (Rampal et al., 2009; Spreen et al., 2011) and increased ice export through narrow channels due to the reduced likelihood of ice arch formation (Babb et al., 2013; Howell et al., 2013). Kwok et al. (2010) showed that reduced ice arch formation and duration in Nares Strait is increasing the advection of MYI from the central Arctic and Lincoln Sea into Baffin Bay. As we have highlighted within this study, changes to the ice flux through Nares Strait have implications for areas downstream that have not typically encountered MYI from the High Arctic and may be facing a new form of marine hazard. Thicker sea ice may become more present at southerly latitudes as ice flux increases through straits that have historically been seasonally blocked by ice arches—a counterintuitive outcome of a warming Arctic and diminishing ice cover.

Acknowledgments

This work is a contribution to the Natural Sciences and Engineering Council of Canada (NSERC) Collaborative Research and Development project: BaySys. Funding for this work was provided by Manitoba Hydro, NSERC, ArcticNet, and the Canada Research Chairs program. Thanks to the captain and crew of the Canadian Coast Guard icebreaker *Amundsen* for their expertise and assistance during our short sampling program off the Northeast coast of Newfoundland. Thanks to the Canadian Ice Service for sharing data and contributing to the development of this paper. The Canadian Ice Service ice chart archive is freely available online. In situ data sets have been registered with the Polar Data Catalogue (#12872)—in situ sea ice geophysical and electromagnetic data from the Newfoundland coast in spring 2017). Thanks to the editor and two anonymous reviewers for their comments and edits that contributed to the improvement of this paper.

References

- Agnew, T., Lambe, A., & Long, D. (2008). Estimating sea ice area flux across the Canadian Arctic Archipelago using enhanced AMSR-E. *Journal of Geophysical Research*, 113, C10011. <https://doi.org/10.1029/2007JC004582>
- Asplin, M. G., Galley, R., Barber, D. G., & Prinsenberg, S. (2012). Fracture of summer Perennial Sea ice by ocean swell as a result of Arctic storms. *Journal of Geophysical Research*, 117, C06025. <https://doi.org/10.1029/2011JC007221>
- Babb, D., Galley, R. J., Asplin, M. G., Hochheim, K., Lukovich, J. V., & Barber, D. G. (2013). Multiyear Sea ice export through Bering Strait during winter 2011/12. *Journal of Geophysical Research: Oceans*, 118, 5489–5503. <https://doi.org/10.1002/jgrc.20383>
- Bourke, R. H., & Garrett, R. P. (1987). Sea ice thickness distribution in the Arctic Ocean. *Cold Regions Science and Technology*, 13(3), 259–280. [https://doi.org/10.1016/0165-232X\(87\)90007-3](https://doi.org/10.1016/0165-232X(87)90007-3)
- Canadian Ice Service (CIS) (2011). Sea ice climatic Atlas for the East Coast 1981–2010. <http://www.ec.gc.ca/glaces-ice/default.asp?lang=En&n=AE4A459A-1&offset=2&toc=show>
- Drinkwater, M. R., Kwok, R., Winebrenner, D. P., & Rigno, E. (1991). Multifrequency polarimetric synthetic aperture radar observations of sea ice. *Journal of Geophysical Research*, 96(C11), 20,679–20,698. <https://doi.org/10.1029/91JC01915>
- European Space Agency (2017). Old Arctic Sea ice going down the drain. Retrieved from http://www.esa.int/spaceinvideo/Videos/2017/06/Old_Arctic_sea_ice_going_down_the_drain
- Fissel, D. B., & Tang, C. L. (1991). Response of sea ice drift to wind forcing on the northeastern Newfoundland shelf. *Journal of Geophysical Research*, 96(C10), 18,397–18,409. <https://doi.org/10.1029/91JC01841>
- Haas, C., Hendricks, S., Eicken, H., & Herber, A. (2010). Synoptic airborne thickness surveys reveal state of Arctic Sea ice cover. *Geophysical Research Letters*, 37, L09501. <https://doi.org/10.1029/2010GL042652>
- Han, G., Colbourne, E., Pepin, P., & Xie, Y. (2015). Statistical projections of ocean climate indices off Newfoundland and Labrador. *Atmosphere-Ocean*, 53(5), 556–570. <https://doi.org/10.1080/07055900.2015.1047732>
- Howell, S. E. L., Wohlleben, T., Daboor, M., Derksen, C., Komarov, A., & Pizzolato, L. (2013). Recent changes in the exchange of sea ice between the Arctic Ocean and the Canadian Arctic Archipelago. *Journal of Geophysical Research: Oceans*, 118, 1–13. <https://doi.org/10.1002/jgr20265>
- Kalnay, E., Kanamitsu, M., Kistler, R., Collins, W., Deaven, D., Gandin, L., et al. (1996). The NCEP/NCAR 40-year reanalysis project, March 1996. *Bulletin of the American Meteorological Society*, 77(3), 437–471. [https://doi.org/10.1175/1520-0477\(1996\)077%3C0437:TNYRP%3E2.0.CO;2](https://doi.org/10.1175/1520-0477(1996)077%3C0437:TNYRP%3E2.0.CO;2)
- Kanamitsu, M., Ebisuzaki, W., Woollen, J., Yang, S.-K., Hnilo, J. J., Fiorino, M., & Potter, G. L. (2002). NCEP-DEO AMIP-II reanalysis (R-2), Nov 2002. *Bulletin of the American Meteorological Society*, 83(11), 1631–1644. <https://doi.org/10.1175/BAMS-83-11-1631>
- Kim, J. W., Kim, D. J., & Hwang, B. J. (2012). Characterization of Arctic Sea ice thickness using high-resolution spaceborne polarimetric SAR data. *IEEE Transactions on Geoscience and Remote Sensing*, 50(1), 13–22. <https://doi.org/10.1109/TGRS.2011.2160070>
- Kwok, R. (2005). Variability of Nares Strait ice flux. *Geophysical Research Letters*, 32, L24502. <https://doi.org/10.1029/2005GL024768>
- Kwok, R. (2007). Baffin Bay ice drift and export: 2002–2007. *Geophysical Research Letters*, 34, L19501. <https://doi.org/10.1029/2007GL031204>
- Kwok, R. (2015). Sea ice convergence along the Arctic coasts of Greenland and the Canadian Arctic Archipelago: Variability and extremes (1992–2014). *Geophysical Research Letters*, 42, 7598–7605. <https://doi.org/10.1002/2015GL065462>
- Kwok, R., Toudal Pedersen, L., Gudmandsen, P., & Pang, S. (2010). Large sea ice outflow into the Nares Strait in 2007. *Geophysical Research Letters*, 37, L03502. <https://doi.org/10.1029/2009GL041872>
- Landy, J. C., Ehn, J. K., Babb, D. G., Thériault, N., & Barber, D. G. (2017). Sea ice thickness in the Eastern Canadian Arctic: Hudson Bay Complex and Baffin Bay. *Remote Sensing of Environment*, 200, 281–294. <https://doi.org/10.1016/j.rse.2017.08.019>

- Lavergne, T., Eastwood, S., Teffah, Z., Schyberg, H., & Breivik, L.-A. (2010). Sea ice motion from low-resolution satellite sensors: An alternative method and its validation in the Arctic. *Journal of Geophysical Research*, *115*, C10032. <https://doi.org/10.1029/2009JC005958>
- Lukovich, J., & Barber, D. (2006). Atmospheric controls on sea ice motion in the southern Beaufort Sea. *Journal of Geophysical Research*, *111*, D18103. <https://doi.org/10.1029/2005JD006408>
- Petty, A. A., Hutchings, J. K., Richter-Menge, J. A., & Tschudi, M. A. (2016). Sea ice circulation around the Beaufort Gyre: The changing role of wind forcing and the sea ice state. *Journal of Geophysical Research: Oceans*, *121*, 3278–3296. <https://doi.org/10.1002/2015JC010903>
- Prinsenberg, S. J., & Peterson, I. K. (1992). Sea-ice properties off Labrador and Newfoundland during LIMEX '89. *Atmosphere-Ocean*, *30*(2), 207–222. <https://doi.org/10.1080/07055900.1992.9649438>
- Prinsenberg, S. J., Peterson, I. K., & Holladay, S. (1996). Comparison of airborne electromagnetic ice thickness data with NOAA/AVHRR and ERS-1/SAR images. *Atmosphere-Ocean*, *34*(1), 185–205. <https://doi.org/10.1080/07055900.1996.9649562>
- Rampal, P., Weiss, J., & Marsan, D. (2009). Positive trend in the mean speed and deformation rate of Arctic Sea ice, 1979–2007. *Journal of Geophysical Research*, *114*, C05013. <https://doi.org/10.1029/2008JC005066>
- Spreen, G., Kwok, R., & Menemenlis, D. (2011). Trends in Arctic Sea ice drift and role of wind forcing: 1992–2009. *Geophysical Research Letters*, *38*, L19501. <https://doi.org/10.1029/2011GL048970>
- Symonds, G. (1986). Seasonal ice extent on the Northeast Newfoundland Shelf. *Journal of Geophysical Research*, *91*(C9), 10,718–10,724. <https://doi.org/10.1029/JC091iC09p10718>
- Tang, C. L. (1991). A two-dimensional thermodynamic model for sea ice advance and retreat in the Newfoundland Marginal Ice Zone. *Journal of Geophysical Research*, *96*(C3), 4723–4737. <https://doi.org/10.1029/90JC02579>